GEOPHYSICAL RESEARCH LETTERS, VOL. 34, L16303, doi:10.1029/2007GL030003, 2007

Post-glacial sediment load and subsidence in coastal Louisiana

Erik R. Ivins,[1] Roy K. Dokka,[2] and Ronald G. Blom[1]

Received 13 March 2007; revised 14 June 2007; accepted 17 July 2007; published 17 August 2007.

[1] Sea level rise in the Gulf of Mexico has occurred at a rate of 1.8–2.2 mm/yr during the 20th century, or nearly the same as observed globally due to combined steric and water mass changes. Tide gauges in coastal Louisiana, however, record a substantially larger rate of rise and while a number of causal mechanisms may be responsible, their specific contribution is poorly understood. Using a realistic viscoelastic Earth model, detailed geologic parameters for south Louisiana and new GPS data, we demonstrate that Holocene sedimentary loading in the Gulf and Mississippi River delta is capable of contributing to 1–8 mm/yr of subsidence over areas of $30–0.75 \times 10^3$ km^2. **Citation:** Ivins, E. R., R. K. Dokka, and R. G. Blom (2007), Post-glacial sediment load and subsidence in coastal Louisiana, *Geophys. Res. Lett.*, *34*, L16303, doi:10.1029/2007GL030003.

1. Introduction

[2] Although the Louisiana coast is far removed from the former ice sheet centers, the waxing and waning of Quaternary glaciations have affected the region through large sea level excursions and fundamental changes in routing of sediments into the Gulf of Mexico. The retreat of the Laurentide ice sheet following last glacial maximum (LGM) produced widespread solid Earth deformation during and after ice sheet demise associated with the Bölling/Allerød interstadial (14–12 ka) warming event. Direct response in the Gulf region, however, has long since faded away. Recent glacial isostatic adjustment (GIA) models calibrated by geodetic data show that the long wavelength peripheral bulge which encircles crustal rebound has now migrated over 1000 km north from the Gulf coast and the regional residual vertical motions are small ($\leq$0.5 mm/a) at present-day [*Sella et al.*, 2007]. However, response to the loading inundation of $\sim$130 meters of equivalent (or eustatic) sea level rise (ESLR) rise at 21–5 kyr BP and Pleistocene sediment transport deposition and loading to the Gulf cannot be dismissed as possible causes of present-day vertical crustal motion [*Jurkowski et al.*, 1984]. In this paper we model both the sediment and ocean load to test predictions of subsidence to that measured using GPS.

2. Lithospheric Loading

[3] Employing a well-established ESLR curve [*Lambeck and Chappell*, 2001], and assuming ocean volume change during the last 5 glacial epochs, we first construct a regionalized model of ocean loading in the Gulf, Mexico's Pacific coast, and the western Caribbean. Prediction of the resulting vertical crustal velocity for one Earth model is shown in Figure 1. While multilayered models are more realistic, here we employ the assumption of a gravitating Earth with a Maxwell viscoelastic half-space (mantle) and an elastic lithosphere [*Ivins and James*, 1999] since the number of retrievable parameters are commensurate with the spatial fidelity of the geodetic data. The model with ocean loading predicts crustal velocity exceeding 0.5 mm/a in some Gulf locations and uparching patterns adjacent to the load, such as in south central Mexico. However, the northern Gulf coast tends to be near a zero contour in the solution. This nodal feature, and the pattern in general, is similar to the computational predictions of recent full spherical calculations [*Mitrovica et al.*, 2001]. We also examined sedimentary loading in the Gulf of Mexico, a part of which may be sourced directly to the Canadian Shield [*Kennett and Shackelton*, 1975]. Although a deposition record is preserved in the shelf edge of the Gulf Coast, extensive reworking, caused, in part, by $\sim$130-meter sea level excursions [*Roberts*, 1997; *Coleman et al.*, 1998], prevents assembly of a complete Pleistocene sedimentation record. Decade long estimates of the rate of deltaic deposition [*Corbett et al.*, 2004] are about 1.3–2.0 cm/yr and coastal near-river sedimentation rates are comparable (13–20 m/ka), substantially larger than are late Cenozoic Gulf Basin-wide rates [*Galloway and Williams*, 1991] (0.1–2 m/ka). Deposition was likely highest during the runoff phase of glacial-interglacial transitions, with rates 4–8 times larger than the present-day [*Teller*, 1990]. A deposition rate of 1.8–2.5 m/ka at distances more than 200 km from the coastline during the post-glacial transition period is both consistent with estimates and proved sufficient for crustal motion predictions. Near-delta, post-glacial transition rates are roughly 10 m/ka. From the beginning of model Sangamonian time ($\approx$610 ka) the total mean sedimentation assumed for the deltaic and near-shore zones is $\simeq$1.1 m/ka.

[4] Sediment loading rates varied in space and time in the model and essentially used estimates of the sediment flux for each of three climate regimes: glacial, interglacial and glacial-interglacial (post-glacial) transition times. Increased hydrological flow through the Mississippi catchment basin delivered runoff to the Gulf during the last glacial transition at a rate, R, of order 3×10^3 km^3 a^{-1} [*Teller*, 1990], or about 0.1 Sv (10^6 m^3 s^{-1}). The ratio of sediment transport flux, S, to runoff, R, is called the efficiency, E_s = S/R. The parameters may be evaluated from measurements at the Three Gorges Dam on the Yangtze River in China [*Yang et al.*, 2005] ($E_s^Y \simeq 0.55 \times 10^3$, $S^Y \simeq 0.425$ km^3 a^{-1}). Using a scale-up factor for the deglacial regime, when large flood events drive efficiencies substantially higher [*Tucker and*

[1]Jet Propulsion Laboratory, California Institute of Technology, Pasadena, California, USA.
[2]Center for GeoInformatics and Department of Civil and Environmental Engineering, Louisiana State University, Baton Rouge, Louisiana, USA.

0094-8276/07/2007GL030003$05.00

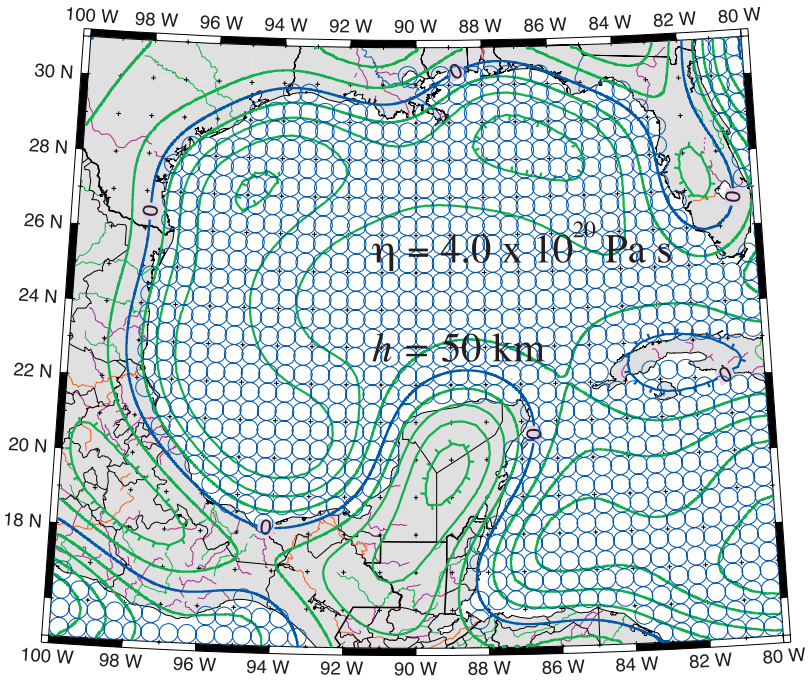

Figure 1. Grids and ocean loading induced present-day vertical motion. Contours are 0.1 mm a^{-1}.

Slingerland, 1997], we set the model E_s to about double the Yangtze value, such that model S = 3.66 km^3 a^{-1}.

[5] Laurentide Ice Sheet retreat produced huge volumes of meltwater that were transported to the continental shelf of the Gulf [*Corbett et al.*, 2004] during 21–13 ka. An ice dam that blocked meltwater flooding through the St. Lawrence River passage broke at about 13 ka and the rate of Gulf-directed sediment transport dropped precipitously, from about 4 × 10^3 to about 1.7 × 10^3 km^3/ka [*Teller*, 1990]. The bulk of the sediments transported to the Gulf region are reworked deposits, initially within the Mississippi catchment basin at the end of LGM. The total mass transported to the Gulf in our 6.1 × 10^5 year model simulation is 4.4 × 10^5 Gt (1 Gt = 1 Giga tonne), an average rate of 0.73 Gt a^{-1}. This is roughly 3–4 times the present-day estimate for the Mississippi River [*Ludwig and Probst*, 1998]. Again, this is consistent with the higher efficiency and runoff rates during the glacial-interglacial transition intervals [*Tucker and Slingerland*, 1997].

[6] A basic characteristic of regional Holocene sedimentation is 'delta switching', a systematic diversion of sediment associated with fundamental shifts in the course of the river. Switching occurs every 1–2 thousand years, and results in deposition of delta lobes of about 35 m in thickness [*Coleman et al.*, 1998]. The simulated Holocene is guided by the switching history [*Stapor and Stone*, 2004; *Otvos and Giardino*, 2004], modern rates of deposition [*McManus*, 2002], and lobe thicknesses [*Coleman et al.*, 1998]. Holocene deposition is non-steady in character, as there are megafloods that can transport sediment throughout the Gulf region [*Brown et al.*, 1999]. Riverine sediment continues to be flushed toward the Gulf after deglacial termination phase, especially during early Holocene time. The 10,000-yr average mass transport rate assumed is 0.68 Gt a^{-1}. The later Holocene deposits are more concentrated due to the virtual cessation of ESLR at about 6–7 ka [*Milne et al.*, 2005]. Table 1 summarizes the volumes assigned to each lobe phase.

3. Present-Day Vertical Crustal Response

[7] Upper mantle viscosity primarily controls the amplitude of the geodetically measured isostatic response to past loading events. It is the integrated "memory" of the sedimentary loading sequences that lies at the heart of the load response model for associated present-day vertical motions in southern Louisiana. For regionalized isostatic modelling, large lateral viscosity variation must be considered [*Nakada and Lambeck*, 1991]. Bounds on the upper mantle viscosity beneath Hudson Bay are estimated at 3–7 × 10^{20} Pa s [*Wolf et al.*, 2006; *Sella et al.*, 2007]. Using lateral temperature variations determined by seismology [*Goes and van der Lee*, 2002], we estimate that the thermomechanical lithosphere beneath the Gulf is thinner, possibly by a factor of

Table 1. Volumes Assumed in Holocene Sediment Loading[a]

Lobe	Volume, km^3	Time, ka
Early Holocene		
Salé-Cypremort + Cocodrie[b]	686	9.5 – 6.0
Mid Holocene		
Teche delta (phase 1)	441	6.0 – 4.5
Teche delta (phase 2)	153	4.5 – 3.5
Late Holocene		
St. Bernard delta	408	3.5 – 2.0
Lafourche delta	838	2.0 – 0.5
Atchafalaya-Wax Lake delta[c]	95	0.5 – 0.0
present Bazile lobe (phase 1)	350	1.0 – 0.5
present Bazile lobe (phase 2)	412	0.5 – 0.0

[a]River sediments (narrow conduits in Figure 3a) are not modeled.
[b]Combining the two lobes has negligible consequences to the geodynamical predictions.
[c]Not shown in Figure 3a, but follows a route similar to the Teche phase 1.

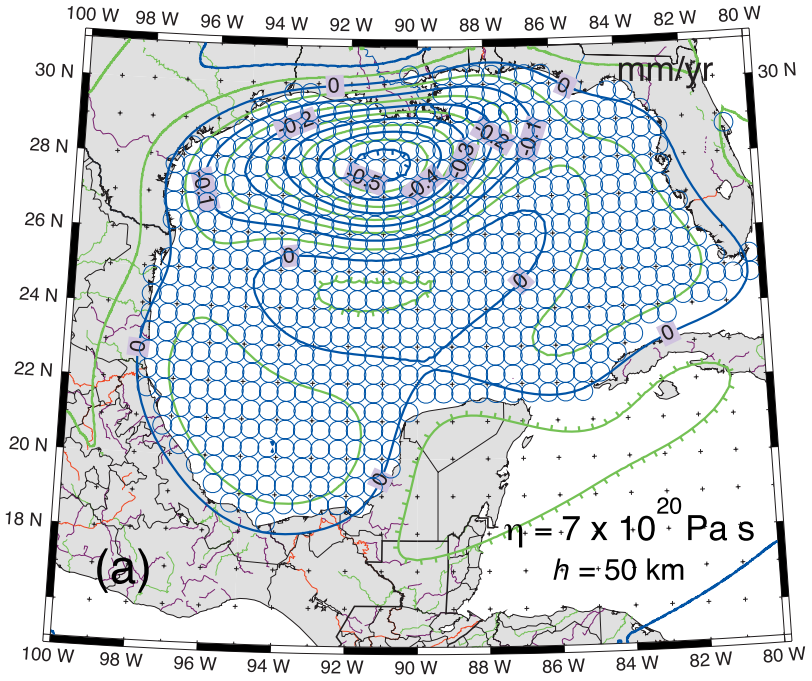

Figure 2. Grids and predicted bedrock subsidence rate in mm a^{-1} assuming Sangamonian glacial cycles with Last deglacial transition (610 to 9.5 ka). No sediment loading younger than 9.5 ka is included. Total sediment transported to the loaded region is $\Delta V = 2.195 \times 10^5$ km^3. All model searches considered lithospheric thickness variability from 40 to 120 km and half-space viscosities from 10^{20} to 10^{21} Pa s.

two, relative to that beneath eastern Canada. Furthermore, the upper mantle viscosity should be near the low end of estimates for Hudson Bay, as these likely represent upper limits on the values for North America.

[8] The forward model assumes an incompressible elastic lithosphere, of density, ρ_l, and rigidity, μ_l on a Maxwell viscoelastic half-space of density, ρ_m, and rigidity, μ_m, and that is hydrostatically pre-stressed [*Ivins et al.*, 2003]. Here we trade off two parameters, lithospheric thickness h, which also influences the exponential decay time constants for the response, and mantle viscosity η. The weaker structure models (smaller h and η) tend to predict stronger geodetic responses with smaller areal extent, whereas stronger structure predicts more widespread deformation, but with smaller amplitude. Emerging from a quick-search procedure is that the viscosity, η, tends to control the subsidence magnitude while h, controls the dominant flexural wavelengths. One example of a relatively large amplitude solution is shown in Figure 2 with the loading limited to sediments that are older than Holocene. Note here that the maximum subsidence is located between basin-wide sedimentation and more local loading near the locus of the Mississippi and Atchafalaya River delta complexes. There are no peripheral uplift features above the 0.1 mm a^{-1} level, unlike ocean loading related motions (Figure 1). The case shown in Figure 2 corresponds to the maximum vertical rate prediction through a search of h and η parameter space. The locus of pre-Holocene Sangamonian load-deformational response is roughly coincident with middle and late Pleistocene depositional centers [*Galloway and Williams*, 1991].

[9] A model solution fit to the GPS data which incorporates a Holocene sediment load, as diagrammed in Figure 3a, plus those for Sangamonian and ocean load cycles is shown in Figure 3b. As before, mechanical strength of the solid Earth substrate is the dominant controlling parameter. Upper mantle viscosity is a critical parameter that influences subsidence amplitudes at coastal sites where geodetic measurements have been reported [*Shinkle and Dokka*, 2004; *Dokka et al.*, 2006]. We select geodetic data from sites located away from active faults and ground water wells, and use only deep set (14–15 meters) monuments to minimize contamination of the subsidence signal by shallow sediment compaction. Comparison to the predictions in Figure 1 illuminates the fact that Holocene loading dominates present-day load-driven subsidence. The model did not consider iterative readjustments to the Holocene loading deposition. We conclude that sediment load has a significant influence that must be considered in predicting the rate of broad-scale, irreversible subsidence and future relative sea level change in coastal Louisiana.

[10] Our informal inversion for η and h indicates that h = 50 km and $\eta = 3 \times 10^{20}$ Pa s are near-optimum values reproducing the observations of vertical land motions in coastal southern Louisiana. Lower h is acceptable, but a parameter search for smaller values of h imply consideration of more complex radial variations and, in turn, enhanced spatial density of the model-constraining geodetic data set. The elastic rigidity of the upper (lithosphere) layer is taken as fixed, $\mu_l = 46.9$ GPa, representative of mid-lower crust. A lower value might also be appropriate; for an upper layer rigidity set to that of consolidated, dry clay [*Helgerud et al.*, 1999], $\mu_l \simeq 6.85$ GPa, for example, the predicted Holocene loading response rates are amplified by about 25%. One possible discrepancy is the vertical rate inferred using relative sea level (RSL) indicators by *Törnqvist et al.* [2006] ($\leq$1 mm a^{-1}) near the site FRAN of Figure 3b. An

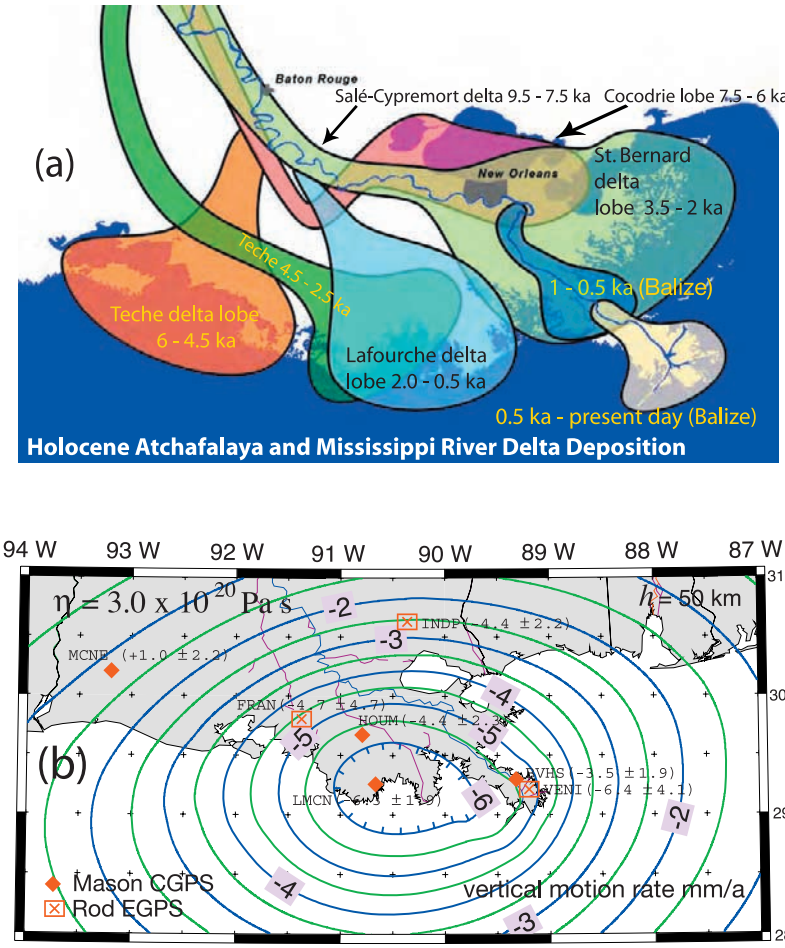

Figure 3. (a) Diagram for Holocene load history and (b) predictions with GPS data for total loading. Model simulation also assumes near shore sedimentation at a rate of 5 mm a^{-1} that extends to about 100 km beyond the delta lobes. See Table 1 for volumes assumed in the simulation. This map is adapted from a number of published sources [e.g., *Roberts*, 1997; *Coleman et al.*, 1998; *McManus*, 2002; *Otvos and Giardino*, 2004; *Stapor and Stone*, 2004]. The red diamonds are for continuous Global Positioning System (CGPS) measurements and episodic ('E') GPS measurements are indicated with red rectangles with cross symbols. (Auxiliary material[1] includes a case for clay-like rigidity and smaller lithospheric thickness, wherein shorter wavelength responses are enhanced.)

improvement in the trend error budget and better control over deep compaction would aid in sorting out this discrepancy.

4. Conclusions

[11] GPS measurements are used to test model vertical motion prediction. The GPS measurements are in reasonably good agreement with our model predictions, both in magnitude and spatial pattern (Figure 3b); a somewhat surprising result in that the Holocene load model tracks the temporal and spatial patterns of Figure 3a, and optimizes only the Earth structure parameters. Predicted vertical motions are of both longer time-scale and wavelength than more localized and temporally punctuated processes that contribute to subsidence, such as fluid withdrawal, salt evacuation and faulting. In order to properly assess present-day Gulf subsidence by lithospheric loading, here we have drawn upon a sufficiently quantitative description of the loads in space and time over the middle and late Pleistocene, though our models are far from being geologically exact. The relative importance of sedimentary loading is linked to the intrinsic solid Earth response times, at various spatial wavelengths. While other factors are clearly also at work [e.g., *Dokka et al.*, 2006; *Dixon et al.*, 2006; *Meckel et al.*, 2006], Holocene sediments provide forces that can explain present-day subsidence at the level of 1–8 mm a^{-1} as observed by GPS. The viscoelastic model has important implications for land-use planning, as the predicted motions are sustained over 100–1000 year time scales. The sediment load-induced, viscoelastic, irreversible subsidence of the city of New Orleans is predicted at about 4.2 mm a^{-1}. When combined with a prediction of 8.8 mm a^{-1} in eustatic rise caused by enhanced polar ice melting [*Overpeck et al.*, 2006], this is a rise of relative sea level in New Orleans of more than one meter in the next 90 years.

[12] **Acknowledgments.** We wish to thank the insightful comments of two anonymous reviewers, editor Eric Calais, and our colleagues Glenn Milne and Volker Klemann. Support for this research was provided to EI and RB by

[1]Auxiliary material data sets are available at ftp://ftp.agu.org/apend/gl/2007gl030003. Other auxiliary material files are in the HTML.

JPL's R.T. & D. Program, to EI by NASA's Interdisciplinary Earth Science Program and by the Solid Earth and Surface Processes Focus Area. RD was supported by grants from the N.S.F. and the Louisiana Board of Regents.

References

Brown, P., J. P. Kennett, and B. L. Ingram (1999), Marine evidence for episodic Holocene megafloods in North America and the northern Gulf of Mexico, *Paleoceanography*, *14*, 498–510.

Coleman, J. M., H. H. Roberts, and G. W. Stone (1998), Mississippi River delta: An overview, *J. Coastal Res.*, *14*, 698–716.

Corbett, D. R., B. McKee, and D. Duncan (2004), Evaluation of short-term sediment dynamics via naturally-occurring radioisotopes in the Mississippi River deltaic region, *Mar. Geol.*, *209*, 91–112.

Dixon, T. H., et al. (2006), Subsidence and flooding in New Orleans, *Nature*, *441*, 587–588.

Dokka, R. K., G. F. Sella, and T. H. Dixon (2006), Tectonic control of subsidence and southward displacement of southeast Louisiana with respect to stable North America, *Geophys. Res. Lett.*, *33*, L23308, doi:10.1029/2006GL027250.

Galloway, W. E., and T. A. Williams (1991), Sedimentation accumulation rates in time and space: Paleogene genetic stratigraphic sequences of the northwestern Gulf of Mexico, *Geology*, *19*, 986–989.

Goes, S., and S. van der Lee (2002), Thermal structure of the North American uppermost mantle inferred from seismic tomography, *J. Geophys. Res.*, *107*(B3), 2050, doi:10.1029/2000JB000049.

Helgerud, M. B., J. Dvorkin, A. Nur, A. Sakai, and T. Collett (1999), Elastic-wave velocity in marine sediments with gas hydrates: Effective medium modeling, *Geophys. Res. Lett.*, *26*, 2021–2024.

Ivins, E. R., and T. S. James (1999), Simple models for late Holocene and present-day Patagonian glacier fluctuations and predictions of a geodetically detectable isostatic response, *Geophys. J. Int.*, *138*, 601–624.

Ivins, E. R., T. S. James, and V. Klemann (2003), Glacial isostatic stress shadowing by the Antarctic ice sheet, *J. Geophys. Res.*, *108*(B12), 2560, doi:10.1029/2002JB002182.

Jurkowski, G., J. Ni, and L. Brown (1984), Modern uparching of the Gulf coastal plain, *J. Geophys. Res.*, *89*, 6247–6255.

Kennett, J. P., and N. J. Shackelton (1975), Laurentide ice sheet meltwater recorded in Gulf of Mexico deep-sea cores, *Science*, *188*, 147–150.

Lambeck, K., and J. Chappell (2001), Sea level change through the last glacial cycle, *Science*, *292*, 679–686.

Ludwig, W., and J.-L. Probst (1998), River sediment discharge to the oceans: Present-day controls and global budgets, *Am. J. Sci.*, *298*, 265–295.

McManus, J. (2002), The history of sediment flux to Atchafalaya Bay, Louisiana, in *Sediment Flux to Basins*, *Geol. Soc. Spec. Publ.*, vol. 191, edited by S. J. Jones and L. E. Frostick, pp. 209–226, Geol. Soc. of London.

Meckel, T. A., U. S. ten Brink, and S. J. Williams (2006), Current subsidence rates due to compaction of Holocene sediments in southern Louisiana, *Geophys. Res. Lett.*, *33*, L11403, doi:10.1029/2006GL026300.

Milne, G. A., A. J. Long, and S. E. Bassett (2005), Modeling Holocene relative sea-level observations from the Caribbean and South America, *Quat. Sci. Rev.*, *24*, 1183–1202.

Mitrovica, J. X., G. A. Milne, and J. Davis (2001), Glacial isostatic adjustment on a rotating Earth, *Geophys. J. Int.*, *147*, 562–578.

Nakada, M., and K. Lambeck (1991), Late Pleistocene and Holocene sea-level change: Evidence for lateral mantle viscosity structure?, in *Glacial Isotasy, Sea Level and Mantle Rheology*, edited by R. Sabadini, K. Lambeck, and E. Boschi, pp. 79–94, Springer, New York.

Otvos, E. G., and M. J. Giardino (2004), Interlinked barrier chain and delta lobe development, northern Gulf of Mexico, *Sediment. Geol.*, *169*, 47–73.

Overpeck, J. T., B. L. Otto-Bliesner, G. H. Miller, D. R. Muhs, R. B. Alley, and J. T. Kiehl (2006), Paleoclimatic evidence for future ice-sheet instability and rapid sea-level rise, *Science*, *311*, 1747–1750.

Roberts, H. H. (1997), Dynamic changes of the Holocene Mississippi River delta plain: The delta cycle, *J. Coastal Res.*, *13*, 605–627.

Sella, G. F., S. Stein, T. H. Dixon, M. Craymer, T. S. James, S. Mazzotti, and R. K. Dokka (2007), Observation of glacial isostatic adjustment in "stable" North America with GPS, *Geophys. Res. Lett.*, *34*, L02306, doi:10.1029/2006GL027081.

Shinkle, K., and R. K. Dokka (2004), Rates of vertical displacement at benchmarks in the lower Mississippi Valley and the northern Gulf Coast, *NOAA Tech. Rep. 50*, 135 pp., U. S. Dep. of Commerce, Washington, D. C.

Stapor, F. W., and G. W. Stone (2004), A new depositional model for the buried 4000 yr BP New Orleans barrier: Implications for sea-level fuctuations and onshore transport from a nearshore shelf source, *Mar. Geol.*, *204*, 215–234.

Teller, J. T. (1990), Volume and routing of late-glacial runoff from the southern Laurentide ice sheet, *Quat. Res.*, *34*, 12–23.

Törnqvist, T. E., S. J. Bick, K. van der Borg, and A. F. M. de Jong (2006), How stable is the Mississippi Delta?, *Geology*, *34*, 697–700.

Tucker, G. E., and R. Slingerland (1997), Drainage basin responses to climate change, *Water Resour. Res.*, *33*, 2031–2047.

Wolf, D., V. Klemann, J. Wunsch, and F. P. Zhang (2006), A reanalysis and reinterpretation of geodetic and geological evidence of glacial-isostatic adjustment in the Churchill region, Hudson Bay, *Surv. Geophys.*, *27*, 19–61.

Yang, S. L., J. Zhang, J. Zhu, J. P. Smith, S. B. Dai, A. Gao, and P. Li (2005), Impact of dams on Yangtze River sediment supply to the sea and delta intertidal wetland response, *J. Geophys. Res.*, *110*, F03006, doi:10.1029/2004JF000271.

R. G. Blom and E. R. Ivins, Earth Sciences Section, Jet Propulsion Laboratory, California Institute of Technology, Mail Stop 300-233, 4800 Oak Grove Drive, Pasadena, CA 91109-8099, USA. (eri@fryxell.jpl.nasa.gov)

R. K. Dokka, Center for GeoInformatics and Department of Civil and Environmental Engineering, Louisiana State University, Baton Rouge, LA 70803, USA.